University of Szeged
Graduate School of Pharmaceutical Sciences
Pharmacodynamics, biopharmacy, clinical pharmacy Ph.D. programme
Programme director: Dr. habil. István Zupkó Ph.D.

Department of Pharmacodynamics and Biopharmacy
Supervisor: Dr. habil. István Zupkó Ph.D.

Judit Molnár

CHARACTERIZATION OF ANTIPROLIFERATIVE ACTIVITIES OF TRIAZOLYL-STEROID DERIVATIVES

Final Exam Committee:
Chairman: Dr. György Falkay
Committee members: Dr. Imre Földesi
Dr. László Puskás

Reviewer Committee:
Chairman: Dr. Piroska Révész
Official reviewers: Dr. Kornélia Tekes
Dr. József Molnár
Committee members: Dr. Gerda Szakonyi
Dr. Zsolt Szakonyi

INTRODUCTION

Since cancerous disorders are the second leading cause of death worldwide, following cardiovascular diseases, improvement of the efficacy of their treatment is currently one of the greatest challenges. A survey of epidemiological data from 184 countries suggested that the global burden of cancer will increase to 23.6 million new cases each year by 2030, an increase of 68% compared with 2012.

In hormone-dependent tumors such as breast, uterine, ovarian, prostate and endometrial cancers, the overexpression of steroid receptors is involved in enhanced cell proliferation. Steroids are a group of endogenous compounds that play versatile roles as anticancer agents. Enzyme inhibitors such as steroid sulfatase inhibitors, aromatase inhibitors (AIs) and 17β-hydroxysteroid dehydrogenase inhibitors, and ligands compete with endogenous hormones for estrogen receptor (ER) such as antiestrogens (selective estrogen-receptor modulators (SERMs) and selective estrogen-receptor downregulators (SERDs)).

Estrogens are widely recognized as factors for tumor growth, mainly in breast cancer. The natural product 2-methoxyestradiol (2ME) is a major estradiol metabolite, the process of the metabolism of estradiol is the same in males and females and it is catalyzed by catechol-*O*-methyltransferase. 2ME has no estrogenic activity and numerous studies showed its anticancer properties (antiproliferative, proapoptotic and cytotoxic activities) and possible cardiovascular benefits.

Plants are among the most varied and promising sources of new anticancer agents and steroids can also be found in them. Natural products are playing a rapidly increasing role in finding the lead candidates for the development of chemotherapeutic agents. They offer a valuable source of compounds with a wide variety of chemical structures with biological activities, and provide important prototypes for the development of novel drugs. Cardiac glycosides are natural steroids, derived from digitalis species. Besides the cardiologic activities of digitoxin and digoxin, these steroids also have an anticancer activity. Compounds containing triazole ring represent a wide range of biological and pharmacological properties. The **t**riazole ring can be found in many biologically active compounds used in therapy such as trazodone, rizatriptan, hexaconazole and alprazolam.

Apoptosis or programmed cell death is a normal component of the development of a multicellular organism. During apoptosis cells die in a controlled manner and apoptotic cells can be recognized by morphological changes. Apoptosis can be activated by various signals from outside and inside the cell, and caspases play a crucial role in this process. Proapoptotic caspases can be divided into two groups, the group of initiator caspases: 2, 8, 9 and 10, and

the group of executioner caspases: 3, 6 and 7. Caspase-8 plays a crucial role in the extrinsic pathway of apoptosis, in which the apoptosis inducing signal derives from death receptors. The intrinsic pathway of apoptosis involves caspase-9 and it is triggered by signals derived from the mitochondrion. The activation of initiator caspases requires binding to specific activator protein. Effector caspases are then activated by these active initiator caspases through proteolytic cleavage for the execution of apoptosis. The G2/M signalling pathway plays an important role in the cycle because this checkpoint regulates the entering of cells to mitosis (M-phase). If the cells have a defective G2/M checkpoint, the cells can enter mitosis before repairing the DNA damage and this leads to uncontrolled cell division with genetic failure. The cell cycle is regulated by cyclins and cyclin dependent kinases (CDKs), and in the case of G2/M checkpoint by the cyclinB-cdc2 (CDK1) complex. DNA damage leads to ATM/ATR kinase activation, resulting in the inactivation of cyclinB/CDK1 complex through the activity of Chk kinase, which phosphorylates and inactivates cdc25, which has an important role in the activation of CDK1 by dephosphorylation

SPECIFIC AIMS

The aim of the present study was to determine the antiproliferative properties of novel, D-ring modified steroid derivatives containing triazole substituent:

Investigation of antiproliferative effects and determination of structure – activity relationship of newly synthesized estranes or androstanes containing substituted triazole ring at position 15, 16, 17 in vitro using human adherent cancer cell lines.

The most effective compounds were selected for additional *in vitro* experiments in order to characterize the possible mechanism of action. These further investigations included cell cycle analysis by flow cytometry, morphological study by fluorescent microscopy after HOPI double staining, caspase-3, -8 and -9 enzyme activity and the expression of cell cycle regulating factors by RT-PCR technique and Western blot study.

Cancer selectivity of the most potent agents was characterized by determining their action on the viability of human fibroblast.

MATERIALS AND METHODS

Chemical structures of novel, D-ring substituted steroid derivatives containing triazole moiety

The first set of the investigated compounds (**1**–**2**) contained 17α-triazolyl steroid analogues. The tested agents possessed estrone or androstane skeleton and in both series a triazole ring was attached to ring D at position 17.

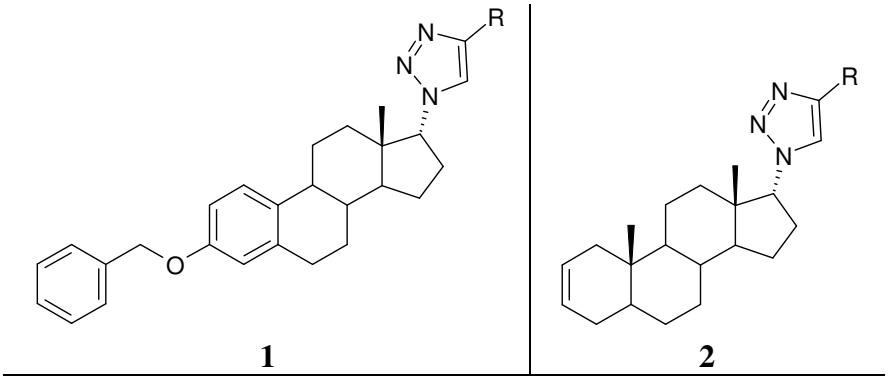

1 **2**

Figure 1. Structures of 17α-triazolyl steroid analogues

The second set of the investigated compounds (**3**–**4**) included 15β-triazolyl-5α-androstane analogues. The tested agents possessed androstane skeleton in which ring A was substituted with acetoxy functions at position 3. The differences between the analogues are the –OH and =O groups at position 17. A triazole ring was attached to ring D at position 15.

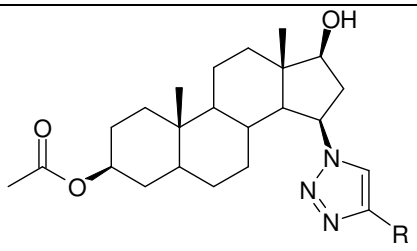

3

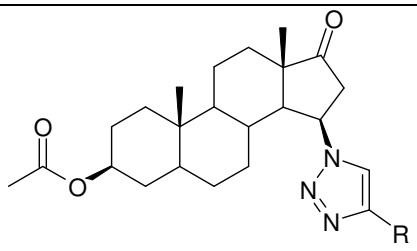

4

3,4	R	**3,4**	R
a	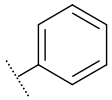	**c**	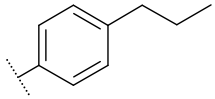
b	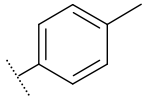		

Figure 2. Structures of the most potent 15β-triazolyl-5α-androstane analogues

The third set of the investigated compounds (**5**–**6**) was composed of 16-triazolyl estrone epimers. The tested agents possessed estrone skeleton in which ring A was substituted with

methoxy function at position 3. A triazole ring was attached to ring D at position 16. The compounds were substituted with different functions on the triazole ring.

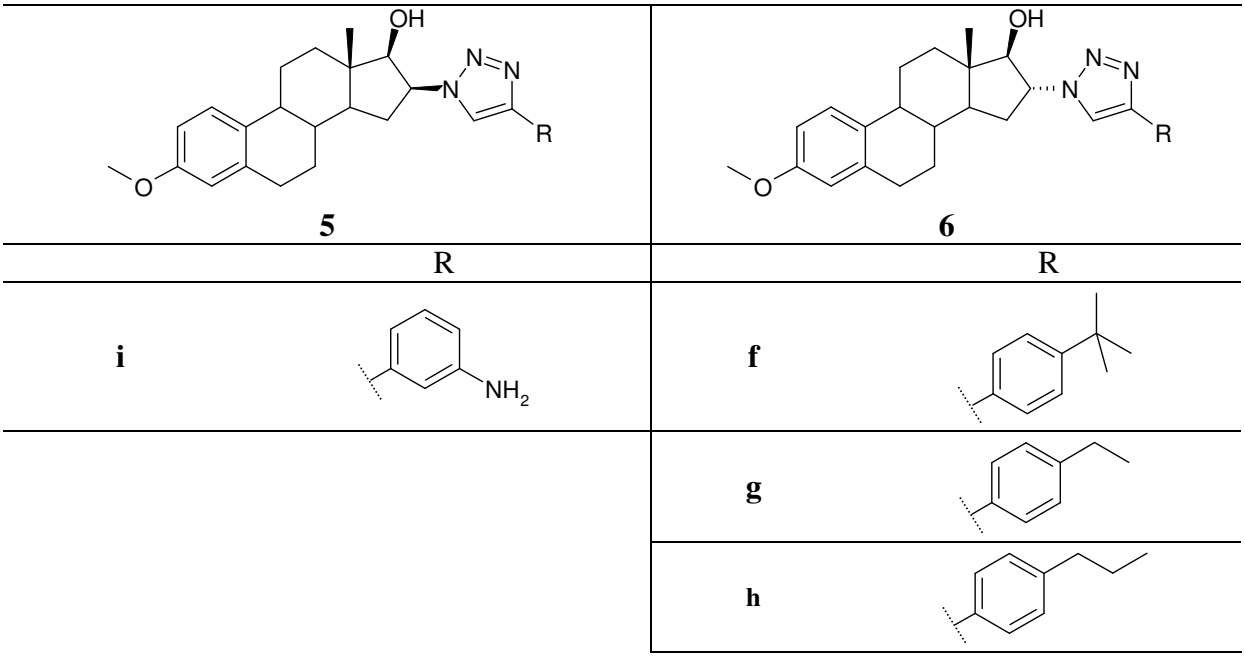

Figure 3. Structures of the most effective16-triazolyl steroid analogues

Tumor cell lines and cell culture

The tested compounds were investigated on HeLa (cervix adenocarcinoma), A431 (skin epidermoid carcinoma), MCF7 (breast adenocarcinoma) and noncancerous MRC-5 fetal lung fibroblast cells. These cells were cultivated in minimal essential medium supplemented with 10% fetal bovine serum, 1% non-essential amino acids and an antibiotic-antimycotic mixture under a humidified atmosphere of 5% CO_2 at 37 ºC.

Determination of antiproliferative effects of the tested compounds

The antiproliferative effects of the tested substances were determined colorimatrically by means of MTT ([3-(4,5-dimethylthiazol-2-yl)-2,5-diphenyltetrazolium bromide]) assay. Briefly, cells were seeded onto a 96-well plate at a density of 5000 cells/well and allowed to stand overnight, after which the medium containing the tested compound was added. After a 72-h incubation period, viability was determined by the addition of 20 µL MTT solution (5 mg/mL). The formazan crystals precipitated during a 4-h incubation were solubilized in 100 µL dimethylsulfoxide (DMSO) and the absorbance was read at 545 nm with an ELISA reader. All *in vitro* experiments were carried out on two microplates with at least five parallel wells. Cisplatin was used as positive control. Sigmoidal dose–response curves were fitted to the measured data in order to determine the IC_{50} values by means of GraphPad Prism 4.0

Cell cycle analysis by flow cytometry

Cellular DNA content was determined by means of flow cytometric analysis, using a DNA-specific fluorescent dye, propidium iodide (PI). The cultured cells were treated with various concentrations of the tested compounds for 24 or 48 h, and the samples were analyzed by FACStar. For each experiment 20,000 events were counted, and the percentages of the cells in the different cell-cycle phases (subG1, G1, S and G2/M) were determined by means of winMDI 2.8.

Double staining with Hoechst 33258 and PI

Cells were seeded into a 96-well plate and incubated with various concentrations of the tested compounds for 24 h. After the incubation period the staining solution was added to the cells. The final concentrations of Hoechst 33258 and PI were 5 and 3 µg/mL, respectively. This staining allowed the identification of intact, early apoptotic, late apoptotic and necrotic cells. HO permeates all cells and makes the nuclei blue. PI is taken up by cells only when the cytoplasmatic membrane integrity has been lost staining the nucleus red.

Caspase-3, -8 and -9 assay

Caspase-3, -8 and 9 activity was determined by using a colorimetric assay kit Ac-DEVD-*p*NA, Ac-IETD-*p*NA and Ac-LEHD-*p*NA serving as substrates, respectively. During the assay, the peptide substrate was cleaved by caspase-3, -8 and -9 resulting in the release of *p*NA (*p*-nitroaniline), which was measured by a microplate reader at an absorbance wavelength of 405 nm. HeLa cells were treated with the tested compounds at 3, 10 and 30 µM for 24 h; untreated cells were used as controls.

Reverse transcription-polymerase chain reaction (RT-PCR) studies

The effects of the tested compounds on the mRNA expression pattern of the markers of apoptosis, such as Bax, Bcl-2 and cyclin-dependent kinase 1 (CDK1), cdc25B, cyclin B1 and cyclin B2, which play a crucial role in the transition from the G2 to the M phase, were determined by RT-PCR in HeLa cells. After a 24-h incubation period, the total RNA was isolated from the cells and cDNS were prepared by the means of reverse transcriptase (RT). Human glyceraldehyde 3-phosphate dehydrogenase (hGAPDH) primers were used as internal control in all samples.

Western blotting studies

To investigate the actions of the most potent compounds on the functions of phosphorylated and total stathmin, protein expression was determined by using Western blot analysis. HeLa cells were treated with the tested agents for 48 h. Whole-cell extracts were prepared protein was subjected to electrophoresis on 4–12% NuPAGE Bis–Tris Gel Proteins were transferred from gels to nitrocellulose membranes, using the iBlot Gel Transfer System Antibody binding was detected with the WesternBreeze Chemiluminescent Western blot immunodetection kit.

RESULTS

Antiproliferative properties of 17α-triazolyl derivatives

The estrone derivatives (**1a**–**j**) have a moderate effect, these compounds elicited less than 60% inhibition of cell proliferation even at higher concentration. The corresponding androstane series (**2a**–**j**) were generally more effective on the cell proliferation. Since most of these analogs exerted a moderate antiproliferative action, no additional experiments were performed.

Antiproliferative properties of 15β-triazolyl-5α-androstanes

The results of the MTT assays led to the selection of **3a**–**c**, **4a** and **4b** for additional experiments in an attempt to elucidate the mechanism of their action.

Antiproliferative properties of 16α-triazolylestrone derivatives

On the basis of their antiproliferative effects, compounds **5i** and **6f**–**h** were selected for further experiments, including characterization of the cancer selectivity. All four steroids exerted limited action on the proliferation of noncancerous fibroblast MRC5. In the cases of **5i** and **6h,** 50% inhibition was not elicited up to 30 μM.

Table 1. Antiproliferative properties of the most potent synthetized compounds

	IC_{50} values (μM)			
	HeLa cells	**MCF-7 cells**	**A431 cells**	**MRC5 cells**
3a	7.70	19.24	20.69	n.d.
3b	9.40	10.28	22.43	n.d.
3c	6.52	>30	>30	n.d.
4a	9.16	1.69	9.69	n.d.
4b	10.27	2.68	10.66	n.d.
5i	13.85	14.88	11.75	>30
6f	5.08	7.88	6.77	17.64
6g	8.69	10.78	10.68	17.07
6h	12.11	>30	>30	>30

Effects of 15β-triazolyl-5α-androstanes on cell cycle

The 24-h treatment with each of these compounds resulted in a concentration-dependent decrease in the number of cells in the G1 phase, and also in an accumulation of the G2/M population (Fig 4). Compound **3c** did not exert any effect on the G2/M phase, but increased the proportion of cells in the synthetic (S) phase. Agents **3a**–**c** and **4a** also resulted in modest but statistically significant increases in the number of hypodiploid (subG1) cells, which are generally regarded as an apoptotic population. This apoptotic proportion became more pronounced after incubation for 48 h.

Effects of 16α-triazolylestrone derivatives on cell cycle

Treatment with the selected estrane analogs resulted in a concentration-dependent increase of subG1 phase cells, which was more pronounced after incubation for 48 h. At the same time, the G1 populations decreased substantially, while the synthetic and G2/M phases exhibited modest, but significant increases (Fig 5).

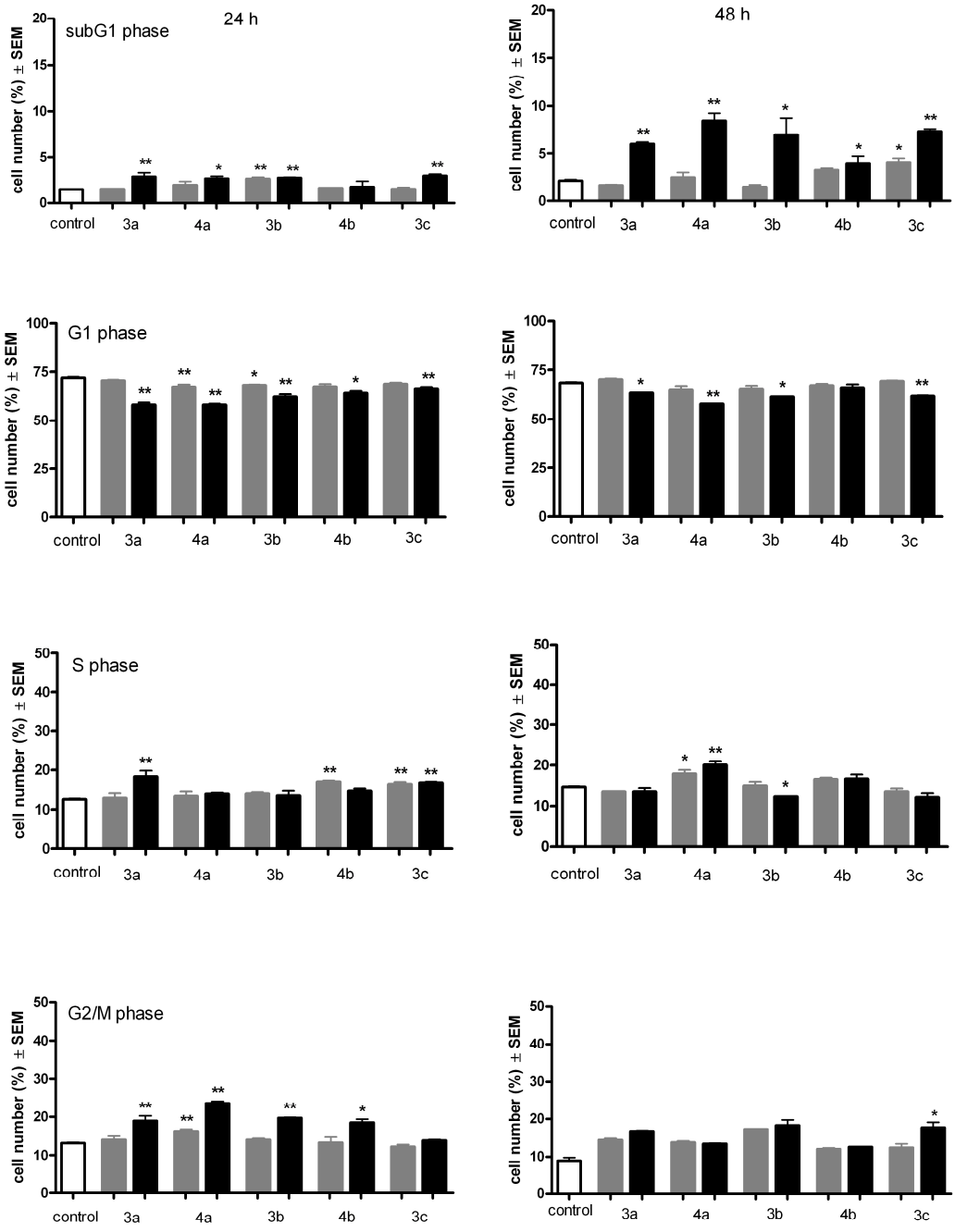

Figure 4. Effects of compounds **3a**-c and **4a-b** on HeLa cell cycle distribution after incubation for 24 (left panels) and 48h (right panels). Grey and black columns indicate 3 and 10 μM, respectively . *and ** indicate $p<0.05$ and $p<0.01$, respectively, as compared with the control cells.

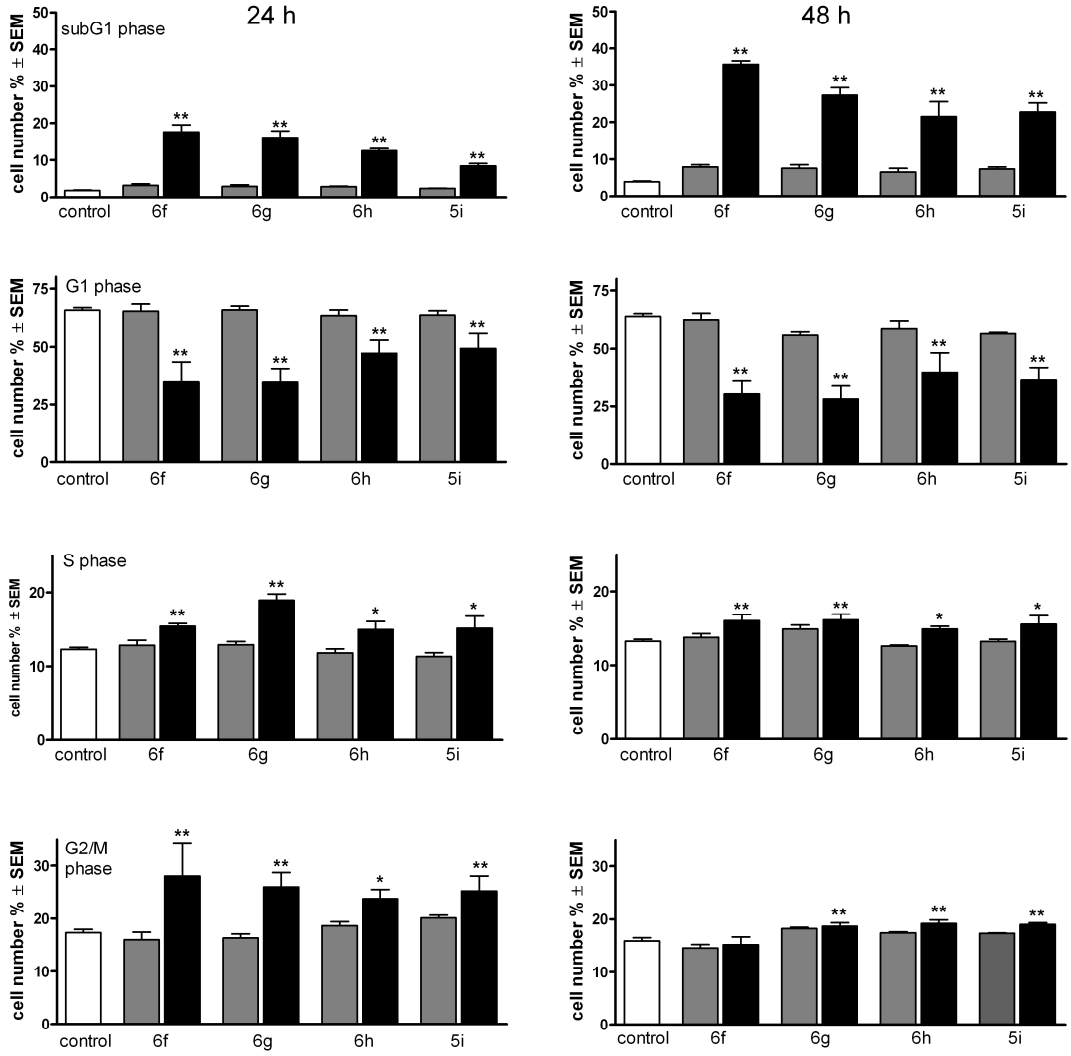

Figure 5. Effects of compounds **6f**, **6g**, **6h** and **5i** on the HeLa cell cycle distribution after incubation for 24 (left panels) and 48 h (right panels). Grey and black columns indicate 3 and 10 μM, respectively. * and ** denote $p<0.05$ and $p<0.01$, respectively, as compared with the control cells.

Morphological studies with 15β-triazolyl-5α-androstanes

Morphological changes such as nuclear condensation, the appearance of apoptotic bodies and increase of the cell membrane permeability were recognized in a concentration-dependent manner as evidence of apoptosis and necrosis. After incubation with 15β-triazolyl-5α-androstanes for 24 h, concentration-dependent increases in nuclear condensation and cell membrane permeability were generally detected, indicated by blue and red fluorescence, respectively (Fig 6).

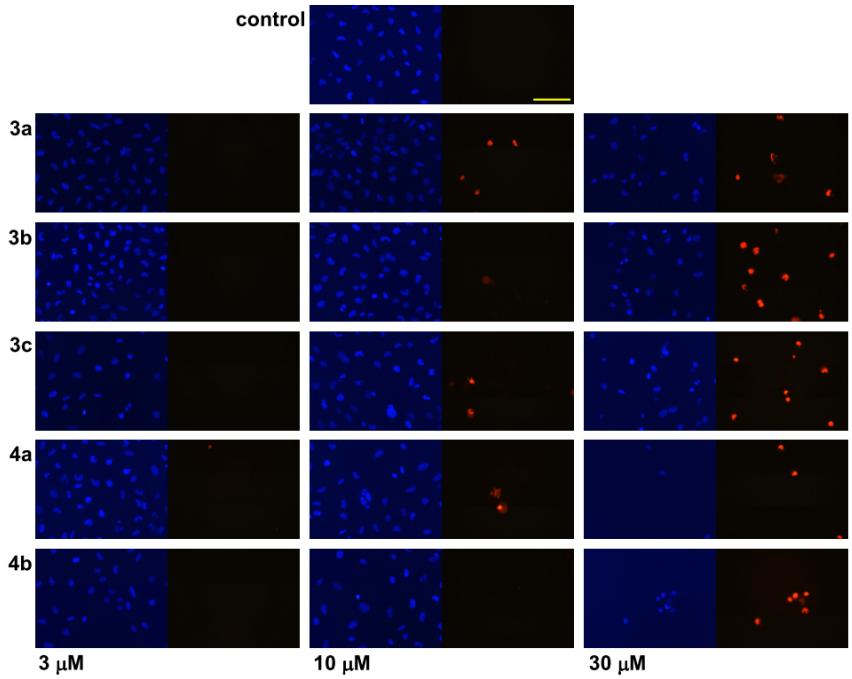

Figure 6. Fluorescence mixcroscopy images of HOPI double staining. Two separate pictures from the same field have been recorded for the two markers. HeLa cells were treated with vehicle (control), or with **3a–c** and **4a–b** at 3, 10 and 30 μM. The blue fluorescence (left panels) indicates HO, and the red coloration (right panels) is a result of cellular PI accumulation. The bar in the HO control picture indicates 100 μm.

Morphological studies with 16α-triazolylestrone derivatives

Four selected steroids from the group of 16α-triazolylestrone derivatives (**5i**, **6f**, **6g** and **6h**) induced early apoptosis, as confirmed by nuclear condensation without increased membrane permeability. Disturbed membrane permeability could be detected in higher concentration without the corresponding nuclear condensation indicating the necrosis-inducing capacity of the agents (Fig 7). Two of the selected steroids (**6f** and **6g**) were tested on MRC5 cells too (Fig. 8). Sparse nuclear condensation was evidenced in fibroblast cells treated with higher concentrations (10 or 30 μM), without marked PI staining.

Caspase-3, caspase-8 and caspase-9 assays

Based on the results of cell cycle analysis and HO-PI double staining, the effects of two selected agents (**6f** and **6g**) on the activities of the apoptotic key enzymes caspase-3, caspase-8 and caspase-9 were determined. Both steroid analogs activated the executive caspase-3 in a concentration-dependent way during a 24-h of incubation (Fig. 9). The activity of the initiator caspase-9 was also significantly increased by both agents. On the other hand, none of the tested agents elicited significant activation of caspase-8.

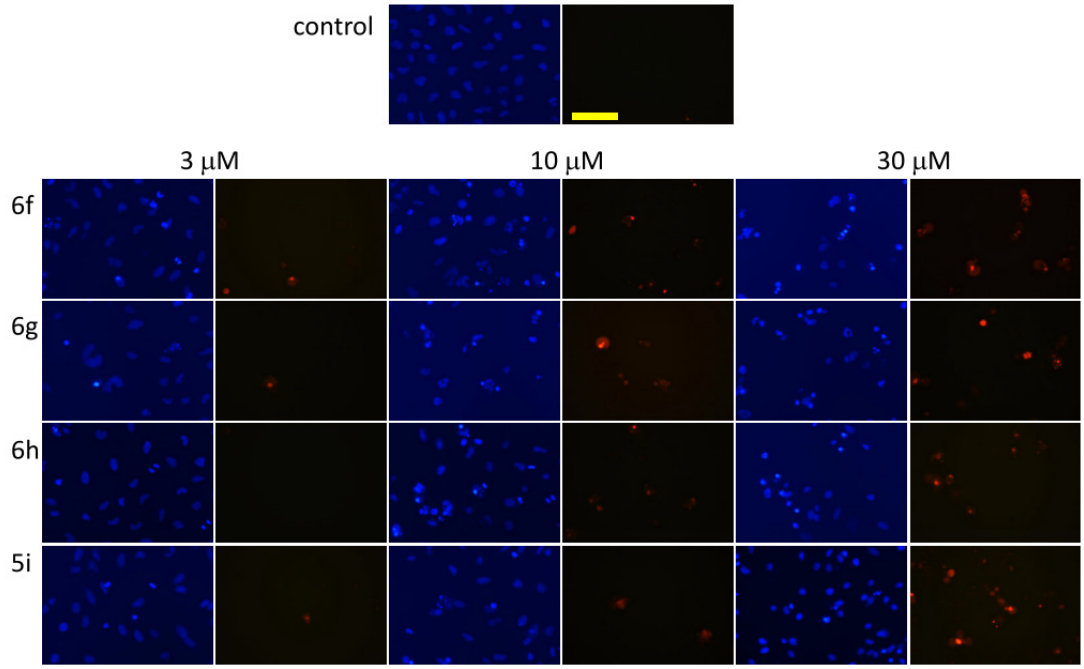

Figure 7. Fluorescent microscopy images of HO-PI double staining. Two separate pictures from the same field were taken for the two markers. HeLa cells were treated with vehicle (control), or treated with **6f**, **6g**, **6h** and **5i** at the indicated concentrations. The blue fluorescence (left panels) indicates HO and the red fluorescence (right panels) is a consequence of PI accumulation. The bar in the PI control picture indicates 100 μm.

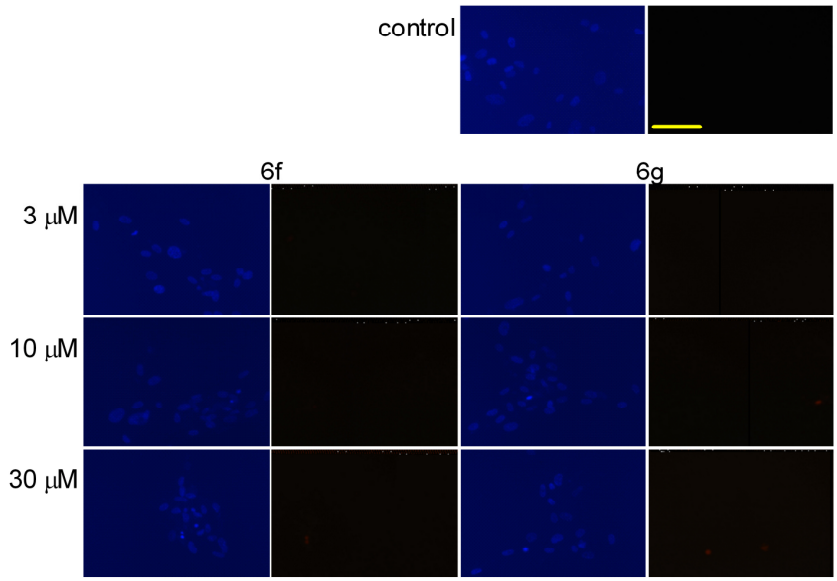

Figure 8. Fluorescent microscopy images of Hoechst 33258-PI double staining. Two separate pictures from the same field were taken for the two markers. MRC5 cells were treated with vehicle (control), or with **6f** and **6g** at the indicated concentrations.

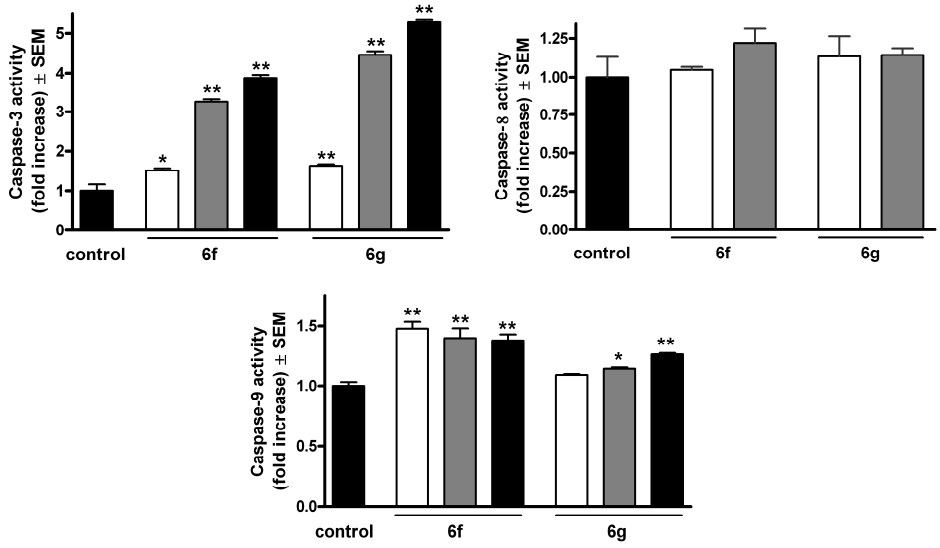

Figure 9. Induction of caspase-3, caspase-8 and caspase-9 activities after incubation with compounds **6f** and **6g** for 24 h. White, gray and black columns denote 3, 10 and 30 μM of the given agent. * and ** denote $p < 0.05$ and $p < 0.01$, respectively, as compared with the control condition

RT-PCR studies

The expressions of the cell cycle regulator factors of the G2–M transition (CDK1, cyclin B1, cyclin B2 and cdc25B) and factors that play key roles in the mitochondrial pathway of apoptosis (Bax and Bcl-2) were determined at the mRNA level by means of RT-PCR. The ratio Bax/Bcl-2 was significantly higher at the higher concentration for the two most effective compounds (Fig. 10). This indicates activation of the mitochondrial pathway of apoptosis. All four selected factors responsible for the G2–M transition were decreased after treatment with the higher concentration (10 μM). Moreover, the expression of cyclin B1 at the mRNA level was significantly reduced even after treatment with 3 μM of **6g** (Fig. 11).

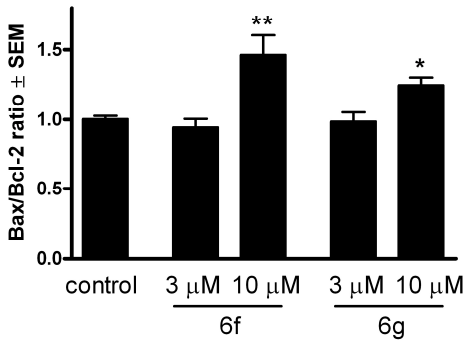

Figure 10. Effects of compounds **6f** and **6g** on the Bax/Bcl-2 ratio after incubation of HeLa cells for 24 h. * and ** denote $p<0.05$ and $p<0.01$, respectively, as compared with the control condition.

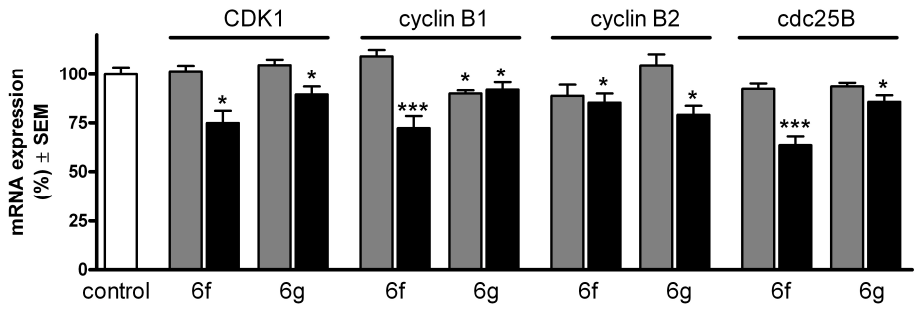

Figure 11. Expression of CDK1, cyclin B1, cyclin B2 and cdc25B at the mRNA level after incubation with 3 (grey columns) or 10 (black columns) μM of compounds **6f** or **6g**. *, ** and *** denote $p<0.05$, $p<0.01$ and $p<0.001$, respectively, as compared with the control condition.

Western blotting studies

In response to a 48-h exposure to 10 μM **6f** or **6g**, the protein expression of phosphorylated stathmin, a microtubule destabilizing protein, was significantly increased severalfold as compared to untreated control cells (Fig. 12). On the other hand, the total amount of stathmin did not display any significant alteration indicating a change in the phosphorylation state of the protein.

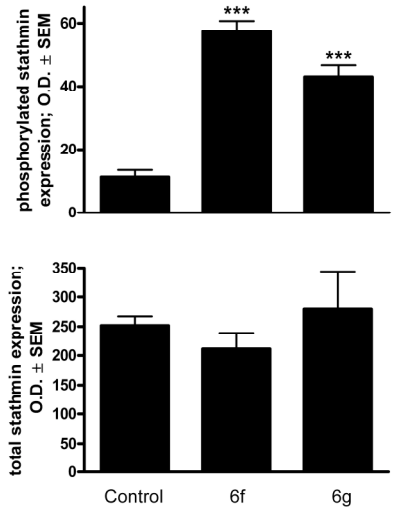

Figure 12. Effects of **6f** and **6g** (10 μM) on the expression of phosphorylated (upper panel) and total (lower panel) stathmin protein in HeLa cells after incubation for 48 h, determined by Western blot analysis. Results are mean values ± SEM of the data on two separate measurements, n = 6. *** indicates $p < 0.001$ as compared with the untreated control cells.

DISCUSSION

The triazole ring is a five-membered heterocycle containing three nitrogen atoms. Triazole compounds such as anastrozole, letrozole are very important antihormonal drugs and a large number of triazole compounds have been exploited as anticancer drugs or candidates in recent years. The structural modification of known anticancer drugs leads to the development of new structural triazole compounds as anticancer agents. A diverse set of innovative compounds with steroidal skeleton bearing the pharmacophore triazole ring on different positions of ring D have been tested for antiproliferative activity. While 17α-triazolyl derivatives exerted limited activities 15- and 16-triazolyl steroids exhibited substantial actions deserving further investigations.

The most potent analogs were subjected to additional investigations in order to describe the mechanisms of their effects. Treatment with each of the four selected molecules (**5i**, **6f**, **6g** and **6h**) for 24 h, even at the lowest concentration (3 μM), resulted in nuclear condensation with minimal or no disruption in membrane permeability, which is a morphological marker of apoptosis. A viability assay and fluorescent staining on intact human fibroblast cells show that two of the four selected molecules (**6f** and **6g**) exhibited higher calculated IC_{50} values against noncancerous than against malignant cells, and did not elicit substantial membrane damage up to 30 μM. A further one of the selected agents (**5i**) did not lead to 50% inhibition of fibroblast growth up to 30 μM, and the fourth (**6h**) proved selective for HeLa cells. Flow cytometry was utilized for a quantitative description of the cell cycle distribution of the treated cells. The most effective agents increased the hypodiploid (subG1) population in a concentration- and time-dependent manner. The reduced DNA stainability is considered to be a consequence of the progressive loss of DNA due to activation of endonuclease and the elimination fragments as part of the self-decomposition during apoptosis. From the aspect of the caspase activation pattern of the two selected compounds, it may be pointed out to that they induce apoptosis via the intrinsic pathway. The activation of caspase-9 seems less pronounced, which is not unusual in view of the fact that this enzyme is the first element in a cascade, while caspase-3 is a terminal element and therefore a product of amplification. Their relation of Bcl-2 and Bax is generally regarded as a marker of the apoptotic–survival balance The higher concentrations of both selected compounds (**6f** and **6g**) resulted in a significant increase in the ratio Bax/Bcl-2, reinforcing the mitochondrial origin of the detected apoptosis. The expressions of CDK1, cyclinB1, cyclinB2 and CDC25B were significantly decreased, indicating that the intervention in the cell cycle machinery is likely to occur at upstream levels.

The presented data demonstrate that estrone may be regarded as a suitable skeleton for the design of innovative antiproliferative drug candidates.

SCIENTIFIC PUBLICATIONS RELATED TO THE SUBJECT OF THE THESIS

1. Frank É, Molnár J, Zupkó I, Kádár Z, Wölfling J: Synthesis of novel steroidal 17α-triazolyl derivatives via Cu(I)-catalyzed azide-alkyne cycloaddition, and an evaluation of their cytotoxic activity in vitro. *Steroids* **76:** 1141-8 (2011)
2. Kádár Z, Molnár J, Schneider G, Zupkó I, Frank É: A facile 'click' approach to novel 15β-triazolyl-5α-androstane derivatives, and an evaluation of their antiproliferative activities in vitro. *Bioorg Med Chem* **20:** 1396-402 (2012)
3. Molnár J, Frank É, Minorics R, Kádár Z, Ocsovszki I, Schönecker B, Wölfling J, Zupkó I: A click approach to novel D-ring-substituted 16α-triazolylestrone derivatives and characterization of their antiproliferative properties. *PLOS ONE* **10:** e0118104 (2015)

ADDITIONAL PUBLICATIONS

1. Molnár J, Ocsovszki I, Puskás L, Ghane T, Hohmann J, Zupkó I: Investigation of the antiproliferative action of the quinoline alkaloids kokusaginine and skimmianine on human cell lines. *Curr Signal Transduct Ther* **8:** 148-55 (2013)
2. Zupkó I, Molnár J, Réthy B, Minorics R, Frank É, Wölfling J, Molnár J, Ocsovszki I, Topcu Z, Bitó T, Puskás GL: Anticancer and multidrug resistance-reversal effects of solanidine analogs synthetized from pregnadienolone acetate. *Molecules* **19:** 2061-76 (2014)
3. Hajdú Z, Hohmann J, Forgo P, Máthé I, Molnár J, Zupkó I: Antiproliferative activity of Artemisia asiatica extract and its constituents on human tumor cell lines. *Planta Med* **80:** 1692-7 (2014)
4. Csupor-Löffler B, Zupkó I, Molnár J, Forgo P, Hohmann J: Bioactivity-guided isolation of antiproliferative compounds from the roots of Onopordum acanthium. *Nat Prod Commun* **9:** 337-40 (2014)